J Musculoskelet Neuronal Interact 2006; 6(2):134-141

Original Article

Hylonome

The importance of the elastic and plastic components of strain in tensile and compressive fatigue of human cortical bone in relation to orthopaedic biomechanics

K. Winwood[1], P. Zioupos[2], J.D. Currey[3], J.R. Cotton[4], M. Taylor[5]

[1]Institute for Biophysical and Clinical Research into Human Movement, Manchester Metropolitan University, UK;
[2]Department of Materials and Medical Sciences, Cranfield University Postgraduate Medical School, Shrivenham, UK;
[3]Department of Biology, University of York, York, UK; [4]Department of Engineering Science and Mechanics, Virginia Tech, Blacksburg, VA, USA;
[5]Bioengineering Science Research Group, School of Engineering Science, University of Southampton, Southampton, UK

Abstract

The longevity, success, or failure of an orthopaedic implant is dependent on its osseointegration especially within the initial six months of the initial surgery. The development of strains plays a crucial role in both bone modelling and remodelling. For remodelling, in particular, strains of substantial values are required to activate the osteoblastic and osteoclastic activity for the osseointegration of the implant. Bone, however, is subject to 'damage' when strain levels exceed a certain threshold level. Damage is manifested in the form of microcracks; it is linked to increased elastic strain amplitudes and is accompanied by the development of 'plastic' (irrecoverable, residual) strains. Such strains increase the likelihood for the implant to subside or loosen. The present study examines the rates (per cycle) by which these two components of strain (elastic and 'plastic') develop during fatigue cycling in two loading modes, tension and compression. The results of this study show that these strain rates depend on the applied stress in both loading modes. It also shows that elastic and plastic strain rates can be linked to each other through simple power law relationships so that one can calculate or predict the latter from the former and vice versa. We anticipate that such basic bone biomechanics data would be of great benefit to both clinicians and bioengineers working in the field of FEA modelling applications and orthopaedic implant surgery.

Keywords: Bone, Strains, Inelastic Behaviour, Fatigue, Damage, FEA, Computer Simulations

Introduction

The most commonly attributed cause of early failure in total hip replacement surgery is either loosening or subsidence of the implant[1-3]. This is seen within the initial six-month post operative period, with revisions currently costing the UK National Health service three times the cost of preliminary surgery[4]. One underlying factor to this issue is changes in apparent density and the mechanical competence of the immediately adjacent cancellous bone, which supports the implant[5-7]. Age-related qualitative changes within the cortical bone tissue itself may compound the bone material/structural problem even further[5,8,9]. After orthopaedic implant surgery the osseointegration of the implant is of major concern and the induction of strain is critical for activation of the bone deposition process[1,10].

Strain levels beyond a certain threshold are also involved in the creation of damage within the tissue in the form of microcracks[9,10]. This damage is associated with inelastic strain behaviour, which shows itself in two ways: in increasing elastic strain amplitudes and in the development of 'plastic' (irrecoverable, residual) strains. Inelastic behaviour has been exhibited by bone in a number of fatigue studies in the past[11-15]. In some of these studies experimental variability was significantly reduced by using 'normalised stress' values (σ/E=normalised stress) and this in a sense also indicated that the results primarily depended on strain, since stress

The authors have no conflict of interest.

Corresponding author: Dr. Keith L. Winwood, Institute for Biophysical & Clinical Research into Human Movement, Manchester Metropolitan University, Hassall Rd, Alsager, ST7 2HL, UK
E-mail: K.Winwood@mmu.ac.uk

Accepted 9 February 2006

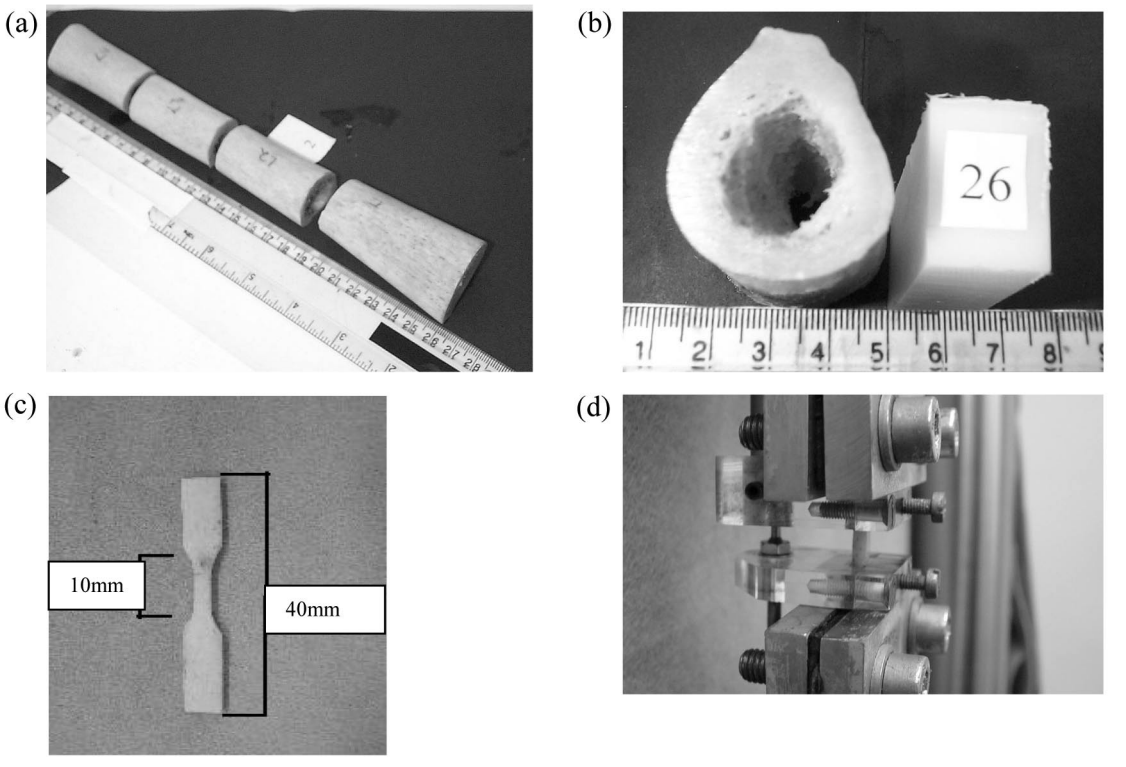

Figure 1. Fabrication and testing of compact bone femoral specimens: (a) whole femur sectioned into four main sections; (b) section of the diaphysis showing high volume of cortical bone from where tensile and compression specimens are harvested; (c) dumb-bell shaped specimens prepared in the longitudinal direction for either tension/compression (5 mm straight gauge length in compression, 10 mm in tension). (d) Grips showing specimen prior to testing with extensometer in place to record the levels of strain during cyclic fatigue (7 mm apart in compression, 12 mm in tension).

over modulus gives a value equivalent to strain. This was a strong indication that strain levels were as influential in determining the outcome in fatigue tests as they had been shown to be in quasistatic loading modes[13,16].

Such inelastic events increase the likelihood for the implant to subside or loosen. Mechanical changes in bone material characteristics alter subsequently the patterns of strain around the implant and cause a redistribution of stresses[15]. One may argue, therefore, that strain levels[1,10] may: (i) play a dominant role in the remodelling process, (ii) provide well understood threshold levels for the development of further damage, and (iii) accordingly regulate the absorption and deposition of newly synthesized bone tissue (via the remodelling process).

The ultimate goal of examination of the inelastic phenomena associated with bone damage and fracture is to fully understand these complex interactions and use them to predict the ultimate course of failure, or more importantly to prevent such failure. This knowledge can be combined with finite element analysis to create realistic models of bone and implant systems[17]. A comprehensive finite element simulation would be of use to implant design, and in the long-term pre-surgical clinical evaluation. Preliminary FE models under simple loads and geometries to predict fatigue failure have been presented, but the experimental knowledge needed for accuracy is lacking. This work presents a portion of the valuable information needed for such simulation.

Materials and methods

Specimens from five female cadaveric femurs (53, 54, 67, 74, 79 years old) and one male (55 years old) were collected, with full ethical approval and relatives' permission and stored at -20°C prior to testing. This tissue was donated after consent for transplantation purposes, and therefore it originated from otherwise healthy individuals with no known reported metabolic bone tissue conditions. Tensile and compressive fatigue specimens were harvested from the diaphysis region in the longitudinal direction and shaped into dumb bell specimens (length 40 mm, width ~3 mm, thickness ~2.5 mm, straight gauge length section 10 mm for tension and 5 mm in compression; Figure 1). All specimens were sanded and polished by using carbide papers (grade 800-1200 grit) and then polished to a mirror finish by the use of alumina slurry paste (MetPrep Ltd., Coventry, UK, gamma alumina 0.05 μm). Specimen preparation was performed

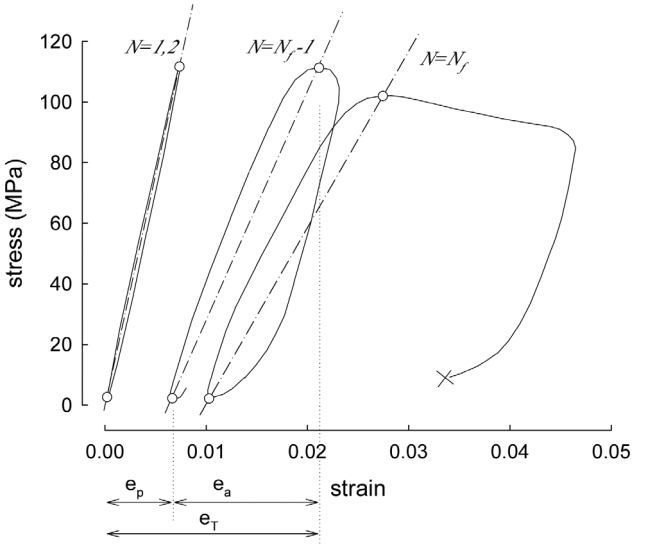

Figure 2. Stress (nominal)/strain (engineering) curves at the start (N=1,2) and at failure in a compression specimen of cortical bone (specimen no F54#19c; N_f cycles to failure=259, stress=110 MPa). The stress and strain values in each cycle were recorded at the peaks of the deformation loops (o) as shown in the figure. The translation in the strain axis (the strains shown here apply to the penultimate cycle N_f-1) is the 'plastic' strain (e_p). Both (e_p) and the increase in the elastic strain amplitude (e_a) is a result of the incipient damage. Total strain is simply $e_T=e_a+e_p$.

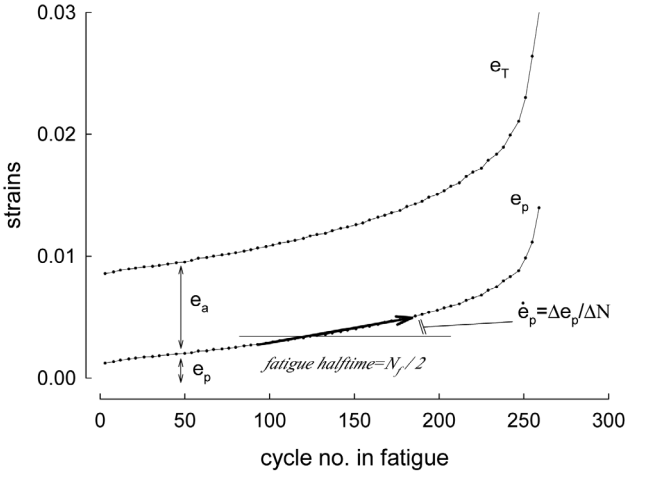

Figure 3. Trends for total strain (e_T) and plastic strain (e_p) with cycle number for the same specimen as in Figure 2. The strain rates were calculated at fatigue halftime=N_f/2, as shown, to produce average representative rates for the whole trace from N=1 to N_f.

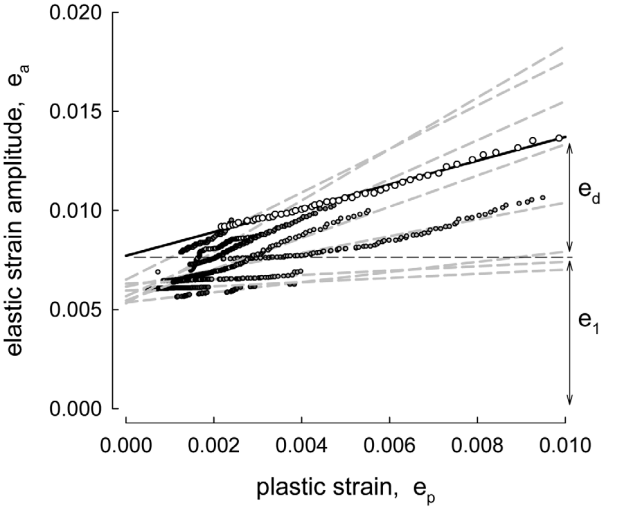

Figure 4. The behaviour of elastic strain amplitudes (e_a) vs. 'plastic' strain (e_p) for all 9 specimens tested in compression from the same donor (female 54 years old) of Figures 2 and 3. Linear regression lines have been fitted to each specimen (dashed grey lines). The intercepts on the y-axis at the start of the fatigue tests, when for e_p=0, are practically the elastic strain amplitudes encountered in the first fatigue cycle (e_1), a result of the applied stress and the modulus of elasticity of each specimen. With fatigue damage a damage strain (e_d) develops so that $e_a=e_1+e_d$ (the solid regression line is for the same specimen as in Figures 2 and 3).

under constant water irrigation, to prevent the production of microcracks or damage to the specimen prior to mechanical testing. Additionally specimens were stained in Fuchsin staining agent (Fisher Scientific®), to verify that no cracks had been induced by the preparation procedure.

Specimens were fatigue cycled sinusoidally at a frequency of 2Hz using a Dartec® HC25 servo-hydraulic testing machine (Zwick Roell Group Ltd, Southern Avenue, Leominster, Hereford, UK) equipped with a 5kN Sensotec® load cell (2080 Arlingate Lane, Columbus, Ohio, 43228, USA) and with specially fabricated grips (Figure 1). Tests were carried out at a constant 37°C and fully immersed in Ringers physiological solution. Strains were recorded by the use of a waterproof fatigue rated extensometer and data collected by using Dartec® Toolkit 96 V4.09 software. In each cycle the strain amplitude (at constant stress amplitude), the plastic strain (which is defined as the irrecoverable translation on the strain axis at zero stress), the cycle number, the time, and the peak load values (for verification) were recorded as entry rows and stored into a spreadsheet format in real time. Every so often (in practice at cycle numbers that followed a power law of 3 increment, N=1,3,9,27...) the full load extension data was recorded at a sampling frequency of 500Hz in order to produce the full load/extension loops at certain points of the fatigue lifetime to demonstrate the qualitative changes in the load/extension behaviour. More details of this set up were presented in Cotton et al.[18,19].

Failure was defined by either the complete rupture of the specimen (as in tension), or at the point where the specimen could not further sustain the cyclically imposed level of stress

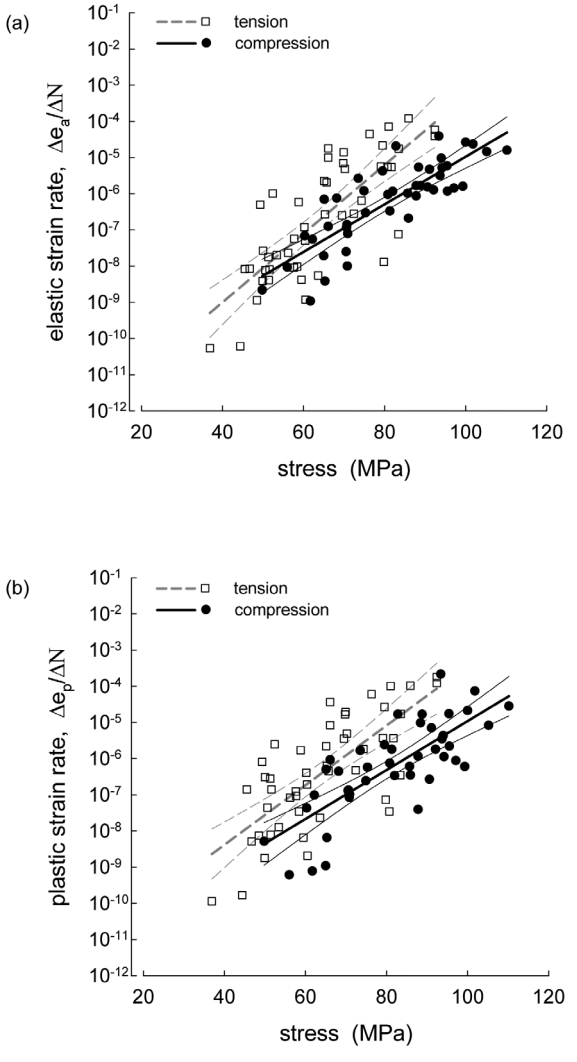

Figure 5. The behaviour of (a) elastic strain rate $\Delta e_a/\Delta N$ and (b) plastic rate $\Delta e_p/\Delta N$ as a function of stress for tension and compression. Least square regression lines with their 95% confidence intervals.

and exhibited high levels of strain. In the case of compression some stress was still transferred through the material from one set of grips to the other via a ligament area of crushed tissue. Typical stress/strain cycles are shown in Figure 2, where also the various components of strain are defined.

For the benefit of definition we have to add that there is no universally accepted terminology pertaining to the inelastic strain components in bone. The translation along the strain axis at zero stress resembles plasticity, but it is not plasticity as the strains recover with time given, and upon relieving the applied stress. The terms therefore 'plastic'[20], 'irrecoverable'[21], or 'permanent'[18] are all poor attempts to describe this complex phenomenon. Equally unsuccessful are the phenomenological terms 'creep strain'[19], or 'strain drift'[22]. Creep is the strain drift associated with constant application of stress and it has been shown[18] that the residual 'plastic' strain observed in tensile fatigue is in fact creep by nature. However, this is not the case universally (as for instance in compression and shear, or even in fully reversed loading in tension) and therefore, the term 'creep' has its shortcomings too.

Having clarified this, and in the present article, we will call the residual strains observed in the inelastic behaviour of bone in fatigue 'plastic' (e_p) to accompany the universally accepted term 'elastic' (e_a) and we emphasize that we make no associations or assumptions as to the cause or the true nature of these residual strains. The rate (with cycle number) by which the 'plastic' strain develops is $\Delta e_p/\Delta N$. The rate by which the elastic strain amplitude increases is similarly $\Delta e_a/\Delta N$ and when the stress amplitude $\Delta\sigma$ is kept constant (as in the present tests) $\Delta e_a/\Delta N$ also relates to the development of damage (usually expressed via a decrease in elastic modulus).

Statistics and curve fitting were performed by using either Minitab (v.13, Minitab Inc, State College, PA 16801-3008, USA), Excel (2002-SP3, Microsoft Corp.) and SigmaPlot (v.8.02, SPSS Inc. Chicago IL, USA) software.

Results

Figure 3 shows the traces of elastic and plastic components of strain with cycle number in fatigue for a representative specimen from the 54-year-old female in compression. The traces for plastic strain were qualitatively different in tension from compression. Tension showed a primary phase (between 0-10% of fatigue lifetime for most specimens) where the tissue showed strong transient effects and a curvilinear behaviour; then a secondary phase at mid-fatigue (fatigue halftime=$N_f/2$), which stretched usually up to 90% of lifetime and where the behaviour was reasonably linear; and then a tertiary region (over 90% of lifetime) nearer failure where the increase in strain was rapid and unpredictable. Compression was slightly different in that there was no primary region and there was a gradual accumulation of strains from cycle 1 until failure (as shown in Figure 3).

To calculate the rate (per cycle) of increase of elastic (e_a) and plastic strain (e_p) components, the slopes of the traces were calculated by linear regressions at the mid-fatigue life region ($N_f/2$). This methodology ignores the events at the start of the cycling and at near failure, but it offers a simple way of describing the behaviour via two constants: an intercept strain at the start of fatigue cycling and the rates of strain given by the two slopes $\Delta e_a/\Delta N$ and $\Delta e_p/\Delta N$. One may then chose to examine how these two rates behave as a function of 'stress', 'age', 'loading mode', the 'donor' or other specimen characteristics.

Figure 4 shows the behaviour of the elastic vs. the plastic components of strain against each other. The behaviour was reasonably linear (the linear regressions of Figure 4 have R^2 values between 0.74 and 0.99). Plastic strain starts from a zero value and depending on the applied stress level increas-

No.	Equation	R^2	p	Loading mode
1	Log ($\Delta e_a/\Delta N$) = -12.8 + 0.0949 stress (MPa)	0.62	<0.001	T
2	Log ($\Delta e_a/\Delta N$) = -11.6 + 0.0657 stress (MPa)	0.69	<0.001	C
3	Log ($\Delta e_p/\Delta N$) = -11.7 + 0.0824 stress (MPa)	0.54	<0.001	T
4	Log ($\Delta e_p/\Delta N$) = -11.7 + 0.0676 stress (MPa)	0.60	<0.001	C
5	Log ($\Delta e_a/\Delta N$) = -11.8 + 1093 normalised stress	0.64	<0.001	T
6	Log ($\Delta e_a/\Delta N$) = -11.1 + 761 normalised stress	0.50	<0.001	C
7	Log ($\Delta e_p/\Delta N$) = -10.9 + 978 normalised stress	0.59	<0.001	T
8	Log ($\Delta e_p/\Delta N$) = -11.3 + 787 normalised stress	0.44	<0.001	C
9	Log ($\Delta e_p/\Delta N$) = -0.543 + 0.872 log ($\Delta e_a/\Delta N$)	0.88	<0.001	T
10	Log ($\Delta e_p/\Delta N$) = - 0.036 + 0.997 log ($\Delta e_a/\Delta N$)	0.82	<0.001	C

Table 1. Linear regression relationships between strain rates, stress (MPa) and normalised stress (stress/modulus) of the data in Figures 5 and 6.

es at a faster or slower rate. The elastic strain itself is the sum of the strain amplitude in the first cycle (e_1) and the extra strain (e_d), which accrues because of damage (formulation used by Haddock et al.[15], $e_a=e_1+e_d$). The rate of increase of the elastic strain ($\Delta e_a/\Delta N$) practically equals the rate of increase of damage strain ($\Delta e_d/\Delta N$).

Figure 5a,b show the behaviour of the strain rates versus nominal stress in the 2 loading modes. As strain rates varied by orders of magnitude (very much like the cycles to failure) logarithmic values for strain rates are used here and for the analysis that follows. Stress was used un-logged because the R^2 values of strain rates vs. stress did not improve appreciably when log (stress) was used.

In some cases, as seen in previous publications the variability of the data (R^2) caused by inter-individual variation can be reduced if the strain rates are plotted versus normalised stress (stress/modulus). Table 1 summarises the relationship for strain rates vs. stress (eq.1-4) and normalised stress (eq.5-8) and for $\Delta e_a/\Delta N$ plotted against the plastic rate $\Delta e_p/\Delta N$ for all the data collected here (eq.9-10). Normalised stress did reduce the variability for tension (eq.5 and 7), but did not help in the cases for compression. That may possibly be caused by errors in measuring the modulus accurately, but we have included the relationships here for completeness of discussion.

The difference in the slopes and intercepts of the regressions were analysed[23] and are shown in Table 2. There are practically two cohorts of data on strain rates, one for the tension experiments and one for the compression experiments for all six donors examined here; the slopes of the lines are not significantly different; and the heights of the distributions about the common slope show only that the compression values are slightly below the tension values (lesser values of the respective strain rates for the same level of stress).

An analysis of covariance was performed to determine whether the individual donors had different relationships between stress, and plastic and elastic strain rate. Plastic or elastic strain rate was the response variable, and the six donors were the treatments. Stress was a covariate. Table 3 shows that although there were differences between the individuals the level of stress was of far greater importance in determining plastic or elastic strain rate. We also found that the age of the individuals, added as a second explanatory variable to the regressions numbers 1-4 in Table 1, never achieved significance. This suggests that the relationship between 'stress' and 'strain rates' does not change uniformly with age. This suggestion was also confirmed by analysis of the residuals.

Comparisons	Slopes different?	Heights different?
Elastic strain rate vs. stress	No	Yes, p<<0.001 (C lower)
Plastic strain rate vs. stress	No	Yes, p<<0.001 (C lower)
Plastic strain rate vs. Elastic strain rate	Yes, p=0.05 (T lower)	**

** there is no need to compare heights (intercepts) when slopes are already different.

Table 2. Analysis of the distributions shown in Figures 5a,b and Figure 6. Comparison of slopes and heights[23].

Figure 6 shows the behaviour of the two types of strain rates against each other. The supporting statistics are in Table 1 and in Table 2 (last entry). The two modes completely overlap so that regardless of stress level, 'donor' (by implication also age), loading mode (tension or compression), and specimen (by implication different specimen characteristics such as structure or modulus of elasticity) there is a unique functional relationship leading from $\Delta e_a/\Delta N$ to $\Delta e_p/\Delta N$ and vice versa. Table 2 shows that statistically the slope for tension is lower than for compression, which is practically equal to one. However, the power law relationship for tension is (Table 1, eq.9): *Plastic strain rate* α *(Elastic strain rate)*$^{0.872}$. Since the values are in logs, the value of R^2 is 0.880, so R is 0.938, and the power law for the functional

Loading mode	Strain rate	Donor F/d.f./p	Stress F/d.f./p
Tension	Elastic	7.08/(5,40)/<0.001	141.62/(1,40)/<0.001
Tension	Plastic	3.25/(5,40)/0.015	75.87/(1,40)/<0.001
Compression	Elastic	3.63/(5,37)/0.009	140.37/(1,37)/<0.001
Compression	Plastic	3.03/(5,40)/0.022	90.49/(1,37)/<0.001
F: F-statistics value/d.f.: (m,n) degrees of freedom/p: level of significance			

Table 3. ANCOVA for the effect of 'stress' and 'donor' on elastic and plastic strain rates.

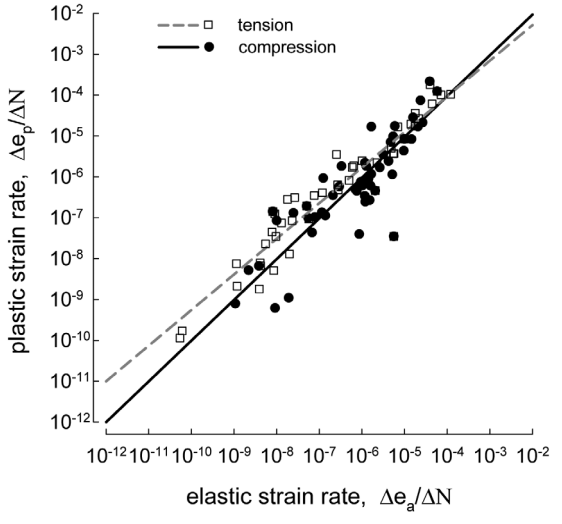

Figure 6. Elastic strain rates $\Delta e_a/\Delta N$ versus plastic strain rates $\Delta e_p/\Delta N$ in fatigue of human cortical bone in tension and compression for all 6 donors examined here. Least square regression lines are also shown.

relationships can be estimated from the slope of the reduced major axis. This is obtained by dividing the regression co-efficient by the correlation co-efficient[24]. This results in an estimate of 0.872/0.938 = 0.930.

Therefore, the power law functional relationship for tension is also very close to unity, and plastic strain rate and elastic strain rate are nearly proportional to each other.

Discussion and conclusions

Bone shows strong inelastic behaviour in fatigue and when stressed beyond certain threshold levels. This inelastic behaviour is accompanied by two main effects: a reduction in stiffness values, and the appearance of residual strains upon unloading. A succession of papers[11,13,16,25-28] have examined such phenomena and speculated as to the practical, evolutionary or even material benefits that may accrue from such behaviour. The essence is that bone '*in vivo*' has been shown to react to such events and via 'remodelling' and 'damage repair' aims to restore itself to a condition as normal as possible. The mechanical signal that bone responds to is by all evidence the level of strain. This has been shown by '*in vivo*' experiments, which specifically regulated strain levels to modify remodelling behaviour and by indirect evidence where strain levels directly affected fracture and damage behaviour.

Considering the importance of strain patterns it is surprising that the behaviour of bone in terms of residual strains upon unloading has not been considered until very recently[29,30]. The present study produced novel information for: (i) the elastic strain amplitude and the residual strains as a function of stress and the cycle number for both tension and compression; (ii) bone tissue material was made available to us from six different individuals spanning ages between 53 to 79 years old, which could illuminate differences between donors of different ages; (iii) there was enough material from each individual (both right and left femurs) to allow testing of paired specimens and record fatigue strength and damage accumulation within each donor and in between donors.

In the analysis we have performed we chose to analyse eventually the strain rate patterns rather than magnitudes of the recorded strains. This was done for two main reasons: (i) simplicity or interpretation; and (ii) ease of utilisation with regard to non-linear Finite Element Analysis (FEA) applications, which use strains assigned on a stepwise basis. In summary: (i) strains e_a and e_p developed in a curvilinear manner as a function of the cycle number (Figure 3) for both loading modes; (ii) the reversible strains e_a were to a good approximation a linear function of the residual strains e_p (Figure 4); (iii) e_p strains were in magnitude a small fraction (30%) of the total strains (e_T) but larger than the damage strains (e_d) in general; (iv) the 'plastic' strain rates were on average 92% of the elastic rates in tension and about 88% of the elastic rates in compression; (v) although the data in Figure 6 is on log/log form and the actual rates of strain range over several orders of magnitude the functional relationship between them is straightforward and may allow simple parameterisation on a stepwise basis for FE models.

What is very interesting is the generic nature of Figure 6. One aspect is the general utility of the strains patterns with regard to modelling and simulation. The other aspect is that

relationships which show such similarity across six different individuals of varying ages, different internal bone architecture, cortical porosity, bone mineral status and so forth, point out that the causal factor of this inelastic behaviour is at the bone matrix level. The influence of factors, which may be regulated by remodelling, such as density, mineral content and architecture have been examined previously with respect to the fatigue strength of bone, but not in terms of the development of damage and accumulation of strains. While fatigue strength is important, under repeated loading of complex structures, the magnitude of damage and strain accumulation will lead to stress redistribution. This may cause subtle differences in initial stress distribution to either magnify or recede, and greatly influence whether implant surgery will turn out to be a success or a failure. Future FE modelling of the stresses around implants will accommodate the material characteristics of the host, the evolution of strains, and redistribution of stresses, to achieve a better result. We expect that this will contribute towards a more successful overall outcome within, in particular, orthopaedic biomechanics.

Acknowledgements

This study was supported by the EPSRC-UK (GR/M59167). The tests were carried out in the Biomechanics Laboratories of Cranfield University Postgraduate Medical School, Shrivenham, UK. The authors would like to thank those bereaved families who kindly donated tissues to be used for the benefit of others.

References

1. Frost HM. Perspectives on artificial joint design. J Long Term Eff Med Implants 1992; 2:9-35.
2. Berry DJ, Harmen WS, Cabanela ME, Morrey BF. Twenty-five-year survivorship of two thousand consecutive primary Charnley total hip replacements: factors affecting survivorship of acetabular and femoral components. J Bone Joint Surg Am 2002; 84A:171-177.
3. Maher SA, Prendergast PJ, Lyons CG. Measurement of the migration of a cemented hip prosthesis in an *in vitro* test. Clin Biomech 2001; 16:307-314.
4. National Audit Office Report by the comptroller and auditor general. Hip replacements: getting it right first time. HC417 Session, 1999/2000, 19th April 2000.
5. Frost HM. A 2003 update of bone physiology and Wolff's Law for clinicians. Angle Orthod 2004; 74:3-15.
6. Taylor M, Tanner KE, Freeman MAR, Yettram AL. Cancellous bone stresses surrounding the femoral component of a hip prosthesis: an elastic-plastic finite element analysis. Med Eng Phys 1995; 17:544-550.
7. Taylor M, Tanner KE. Fatigue failure of cancellous bone: a possible cause of implant migration and loosening. J Bone Joint Surg Br 1997; 79B:181-182.
8. Zioupos P, Wang XT, Currey JD. The accumulation of fatigue microdamage in human cortical bone of two different ages *in vitro*. Clin Biomech 1996; 11:365-375.
9. Zioupos P, Currey JD. Changes in the stiffness, strength and toughness of human cortical bone with age. Bone 1998; 22:57-66.
10. Frost HM. Does bone design intend to minimize fatigue failures? A case for the affirmative. J Bone Miner Metab 2000; 18:78-282.
11. Carter DR, Hayes WC. Compact bone fatigue damage-I. Residual strength and stiffness. J Biomech 1977; 10:325-337.
12. Fleck C, Eifler D. Deformation behaviour and damage accumulation of cortical bone specimens from the equine tibia under cyclic loading. J Biomech 2003; 36:179-189.
13. Zioupos P, Currey JD, Sedman A. An examination of the micromechanics of failure of bone and antler by acoustic-emission tests and Laser Scanning Confocal Microscopy. Med Eng Phys 1994; 16:203-212.
14. Choi K, Goldstein SA. A comparison of the fatigue behavior of human trabecular and cortical bone tissue. J Biomech 1992; 25:1371-1381.
15. Haddock SM, Yeh OC, Mummaneni PV, Rosenberg WS, Keaveny TM. Similarity in the fatigue behavior of trabecular bone across site and species. J Biomech 2004; 37:181-187.
16. Fondrk MT, Bahniuk EH, Davy DT, Michaels C. Some viscoplastic characteristics of bovine and human cortical bone. J Biomech 1988; 21:623-630.
17. Taylor M, Cotton J, Zioupos P. Finite element simulation of the fatigue behaviour of cortical and cancellous bone. Meccanica 2002; 37:419-429.
18. Cotton JR, Zioupos P, Winwood K, Taylor M. Analysis of creep strain during tensile fatigue of cortical bone. J Biomech 2003; 36:943-949.
19. Cotton JR, Winwood K, Zioupos P, Taylor M. Damage rate is a predictor of fatigue life and creep strain rate in tensile fatigue of human cortical bone samples. J Biomech Eng 2005; 127:213-219.
20. Taylor M, Verdonschot N, Huiskes R, Zioupos P. A combined finite element method and continuum damage mechanics approach to simulate the *in vitro* fatigue behaviour of human cortical bone. J Mater Sci Mater Med 1999; 10:841-846.
21. Zioupos P, Winwood K, Cotton J, Taylor M. The development of elastic and 'plastic' strains during fatigue damage accumulation of human cortical bone. Acta Bioeng Biomechan Proc 13th ESB Conference 2002; Wroclaw, Poland.
22. Pattin, CA, Caler, WE, Carter DR. Cyclic mechanical property degradation during fatigue loading of cortical bone. J Biomech 1996; 29:69-79.
23. Snedecor GW, Cochran WG. Statistical Methods. 7th Edition. Iowa State University Press; 1980.
24. Rayner JMV. Linear relations in biomechanics: the statistics of scaling functions. J Zoology (London) 1985; 206A:415-439.

25. Currey JD. Anelasticity in bone and echinoderm skeletons. J Exper Biology 1965; 43:270-292.
26. Bonfield W, Li CH. Anisotropy of nonelastic flow in bone. J Appl Physics 1967; 38:2450-2455.
27. Fondrk MT, Bahniuk EH, Davy DT. Inelastic strain accumulation in cortical bone during rapid transient tensile loading. J Biomech Eng 1999; 121:616-621.
28. Fondrk MT, Bahniuk EH, Davy DT. A damage model for nonlinear tensile behavior of cortical bone. J Biomech Eng 1999; 121:533-541.
29. Winwood K, Zioupos P, Cotton J, Taylor M. The development of 'plastic' strains during fatigue damage accumulation of ageing human cortical bone. Congress of the International Society of Biomechanics, Zurich, Switzerland, July 8-13th 2001.
30. Winwood K. An experimental investigation into the effects of fatigue on human cortical bone. PhD thesis. Department of Materials and Medical Sciences, Cranfield Postgraduate Medical School, Cranfield University; 2003.